



Study of a hardfacing flux-cored wire for arc directed energy deposition applications

Ana Cardoso¹ · Eurico Assunção² · Inês Pires¹

Received: 20 December 2020 / Accepted: 24 September 2021 / Published online: 15 October 2021
© The Author(s), under exclusive licence to Springer-Verlag London Ltd., part of Springer Nature 2021

Abstract

This paper investigates the feasibility of producing hard structures capable of wear resistance by depositing a hardfacing flux-cored wire while using arc directed energy deposition (DED-Arc) as process. The present paper discloses the compatibility of a metal hardfacing flux-cored wire with this technology by deposition of single walls and block fabrication. The deposition of walls and blocks was made using different parameters and deposition strategies, in order to avoid solidification cracking associated with the precipitation of chromium carbides. Macro and microstructural analyses, as well as hardness tests, were carried out to validate the use of this wire with DED-Arc. The use of a grinder for slag removal was also investigated. Withal, the deposition of a 40-layer wall and blocks indicated that a hardfacing flux-cored wire can be used to produce a near net shape part by additive manufacturing. Additionally, gradient properties of additively manufactured metal parts can be achieved by depositing layers of materials with different characteristics and, with DED-Arc, this can be done through the use of different types of metal wire. Thus, studies on the possibility of constructing a bi-metallic part, by DED-Arc, using a low carbon steel (ER70S-6) and the same hardfacing-cored wire were developed, focusing on crack minimization procedures, such as the application of pre-heating. Assessment of metallurgical transformations and mechanical properties were investigated to assure that the material properties were kept. A final multi-metal part was produced with DED-Arc.

Keywords Arc directed energy deposition (DED-arc) · Flux-cored wire · Multi-metal parts · Microstructure · Microhardness · CMT

1 Introduction

Metal additive manufacturing (MAM) processes allow the reduction of costs by decreasing material wastage and time to market. Likewise, these techniques enable the manufacturing of near net shape parts, increasing design freedom and weight saving [1]. Although different AM processes for metallic parts fabrication are available, arc directed energy deposition provides a promising solution for producing medium to large metal parts through layer-by-layer deposition [2]. This technology uses a solid wire as consumable for deposition, managing to achieve high fabrication envelopes and deposition rates [3, 4]. However, DED-Arc

manufactured parts are subject to high heat inputs, which induce high residual stresses and distortions [4]. Therefore, several strategies have been developed to minimize residual stresses, either by post-processing technologies, like thermal treatments, or even by the control of the build-up residual stresses during the deposition, such as the high-pressure inter-pass rolling, optimization of part orientation, back to back building and symmetrical building [5, 6]. Additionally, DED-Arc fabricated parts are likely of medium to low complexity, which inhibits the deposition of some shapes, such as sharp angles and curve shapes with large curvature, due to the large molten pool and shape distortion caused by surface tension [7].

Nonetheless, to this day, a variety of components have been successfully manufactured by DED-Arc, including Ti–6Al–4V spars and landing gear assemblies, aluminium wing ribs, steel wind tunnel models, and cones. Although a variety of materials already produce fine results with this type of additive manufacturing technology, such as aluminium, titanium, and steel alloys, there is still the

✉ Ana Cardoso
ana.s.faria@tecnico.ulisboa.pt

¹ Instituto Superior Técnico (IST), Universidade de Lisboa, Lisbon, Portugal

² European Federation for Welding, Joining and Cutting (EWF), Oeiras, Lisbon, Portugal

need for further investigation on process parameters and to test more materials, in order to strengthen and enlarge the application field of this technology [8–13].

In this context, the present work aims to study the potential of a hardfacing flux-cored wire in DED-Arc, as this material can give rise to parts with high wear resistance. The studied material, the UTP AF Robotic 600 flux-cored wire, presents hardfacing characteristics that may allow the production of wear resistance components [14]. Additionally, as only solid wires have been studied so far, the study of flux-cored wires presents an attractive innovation since this type of wires are associated with high deposition rates and high productivity and could even further reduce lead times, improving productivity and promoting cost savings. Presently, the maximum hardness observed in an additive manufactured part was a tool steel disc with an average hardness of 599 HV [15]. The final aim of this work is to obtain hard near net shape parts deposited with the flux-cored hardfacing wire envisioning high hardness and wear resistance parts. Considering that hardfacing deposited materials are extremely difficult to machine, the successful construction of near net shape structures would vastly spread the DED-Arc range of applications. For the success of this technology, it is required that the produced parts are defect-free and that a good cohesion between layers is achieved, thus metallurgical analysis and hardness tests were made to evaluate the potential of using a hardfacing wire in the manufacture of components by DED-Arc. Also, in order to manage residual stresses and eliminate manufacturing defects, deposition strategies and heat treatment processes were considered [1, 15]. In addition, and envisioning a wide range of applications for such wire, parameters optimization was carried with different thicknesses.

Moreover, the combination between the hardfacing wire and a low carbon steel wire was studied. The intent was to produce multi-material parts, with enhanced characteristics where needed, for instance, increase the hardness on critical areas or allow a greater ductility on less demanding areas, which can contribute to the increase of the part's lifespan and performance, as well as provide greater design flexibility [16]. The fabrication of multi-metal parts can additionally lead to a reduction of the final product cost using, for example, a costless material where no specific requirement is needed and a more expensive one where wear resistance is needed.



Fig. 1 Set up of the experiment: (1) Fronius VR 7000 CMT (cold metal transfer) power source; (2) substrate plates; (3) shielding gas; (4) 6-axis KUKA robot; (5) grinder; (6) jigs for clamping

2 Materials and methodology

2.1 Material

The main used consumable in the present work was a flux-cored wire, denominated as UTP AF Robotic 600, developed by *Voestalpine*. For bi-metal parts, a low carbon steel wire, ER70S-6, was also used. The chemical composition of each wire can be seen in Table 1, where Fe is the balance element. Both consumables presented a 1.2 mm diameter. A shielding gas mixture composed of CO₂ (18%) and Argon (82%) was used for both wires, as recommended by the EN ISO 14175:M21 standard.

Carbon steel plates with 20 mm thickness have been used as substrate to perform the experiments. Extra space was considered for clamping the substrate plate to the welding table. The plates were mechanically cleaned and then fixed on the worktable before the deposition process.

2.2 Equipment

Figure 1 shows the DED-Arc system used in the present research. As also depicted in Fig. 1, substrate plates were

Table 1 Chemical composition of the wire metals, wt%

	C	Mn	P	S	Si	Cu	Cr
UTP AF Robotic 600	0.45	0.4	–	–	3.0	–	9.0
ER70S-6	0.09	1.65	0.012	0.018	0.95	0.35	–

clamped to a welding table with jigs for a stable deposition. For some wall depositions, a grinder was used (explained in Sect. 3.1). Regarding the bi-metal tests, a propane blowtorch and a thermocouple were used in some trials, for pre-heating purposes (as described in Sect. 3.3). Metallographic investigation was performed on a Zeiss microscope. As for the samples' hardness, Vickers hardness tests on the deposited sections were performed using a Struers Duramin Vicker hardness indenter.

2.3 Methodology

In order to obtain the process parameters for this flux-cored wire, a preliminary study was carried out making single beads under CMT operation mode with different combinations of process parameters. The main variable parameters were the wire feed speed (WFS), the travel speed (TS), and the waiting time between layer deposition. The other parameters remained constant through the study, namely the shielding gas, the flow rate that was equal to 18 l/min, and the distance between the contact tip and the workpiece with a value of 18 mm. Subsequently, the study moved to linear wall deposition using the parameters identified in the previous step. Blocks were also built with different deposition strategies, particularly the oscillation, the parallel, and the weaving strategy, as represented in Fig. 2. The same procedure was used to make the two-metal deposits.

Following deposition, the study progressed to sample characterization through microstructural analysis. Eye observation, macro, and microscopic evaluation were employed in order to search for defects, such as porosities, cracks, and lack of fusion. Each set of tests adopted the following procedure: (1) samples cut by electrical discharge machining (EDM), due to the high hardness associated with the hardfacing material;

(2) polishing and etching; (3) macro and microscopy observation using optical microscope; (4) hardness tests.

Regarding polishing procedures, they were performed as follows: the samples were hot polished during 9 min in hot (at 180 °C) and 9 min in cold. After, the samples' surface was grinded following the presented method: grinding with 80, 120, 220, 320, 500, and 1000 grit sandpaper. Several polishing steps were pursued: application of diamond paste of 6 μm , finished with 1 μm . To etch the samples, in the first place, a solution of Nital 2% (98 ml of alcohol and 2 ml of nitric acid) was used to contrast the substrate during 10 s; next, and following the E 407-99 Standard Practice for Microetching Metals and Alloys, the reagent used to etch the deposits was the Vilella (100 ml alcohol, 5 ml hydrochloric acid, and 1 g picric acid).

Micrographs were taken at 50 \times , 100 \times , 200 \times and 500 \times magnification. The indentations on the Vickers hardness tests were carried out along the central line with a load of 1 kg during 10 s, with increments of 1 mm spacing, from half of the substrate to the top of the wall.

3 Results and discussion

3.1 Wall deposition

The majority of the tests were carried out with bidirectional deposition, which allowed to obtain a balanced wall, with a constant height along the wall's length, as can be seen by some of the deposited walls depicted in Fig. 3. The walls were built with 6 layers and 120 mm in length. For the initial trials, 30 s of waiting time were used between layers. However, in subsequent tests, the waiting time had to be

Fig. 2 Deposition strategies: **a** oscillation, **b** parallel, **c** weaving

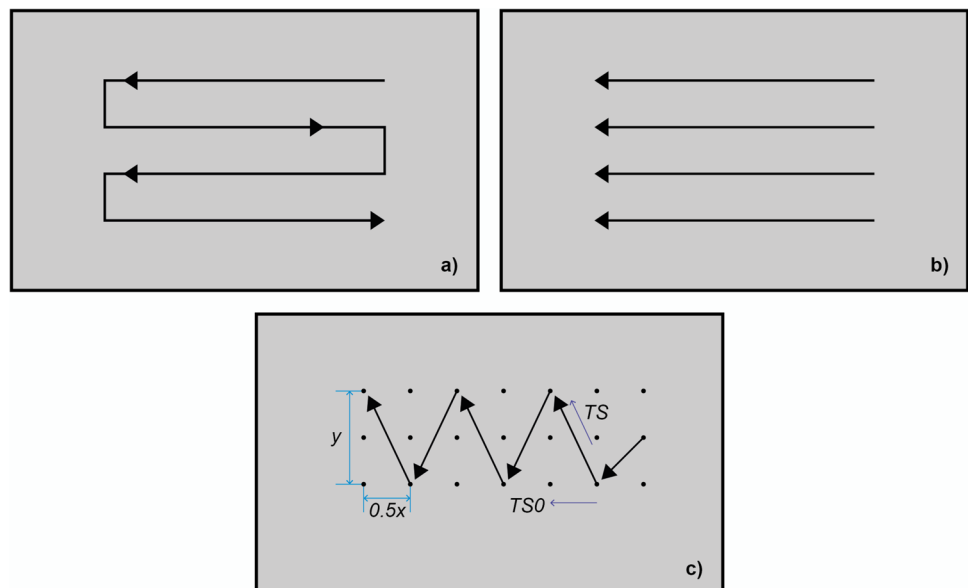




Fig. 3 Example of wall deposition using different parameters

Table 2 Parameters optimization

	WFS (m/ min)	WFS/TS	Thickness (mm)	Total height (mm)	Waiting time (s)
Normal	6.5	21.7	13	10.9	60
Thinner	5	20	10.8	11.2	60
	5	15	9.5	16.3	60
	4	10	7.4	10.0	60
	4	5	4.8	7.7	30
	3	5	4.3	7.4	30
Weaving	5	10	9.2	15.8	180

increased accordingly up to 180 s, in order to give the slag enough time to come off.

Firstly, deposits were made using different parameters in order to obtain a record of workable parameters. With this, different heights and thicknesses were determined in function of the WFS and the TS, which would allow future parts construction with different geometries. The study of parameters for CMT mode has led to the results indicated in Table 2, considered to be the best results by visual inspection due to the regular superficial aspect of the deposit. The parameters that provided the better results for the weaving deposition technique can also be found in Table 2. From the data collected in Table 2, it is possible to understand that to produce thinner walls, the WFS should decrease or the TS should increase, in order to lower the ratio WFS/TS. However, it is necessary to

compromise to produce sound deposits, so even if it's possible to decrease the wall thickness greatly by increasing the TS, it is also necessary to balance the WFS (or else walls will be deposited with irregular thickness, as demonstrated by the fourth wall, counting from the bottom to the top, in Fig. 3). Also, when the thickness is lower, and subsequently the TS is higher, the waiting time needed for the slag to come off also decreases.

The maximum deposition rate obtained in these tests, corresponding to the “normal bead” parameters, was 4.5 kg/h. Although close, this value did not surpass the deposition rate found in literature of 5 kg/h for the AISI 316L, for example. However, it still provides a higher deposition rate compared with titanium and nickel-based alloys, which present a deposition rate of 2.5 kg/h [4, 17].

As flux-cored wires produce slag, a fundamental part of this research focuses on the effect that the slag could have on the integrity of the weld. Therefore, two samples with six layers each were built using the same parameters, however in one of the tests manual grinding between layers, with a Dremil, was used to remove any traces of slag, while in the other sample just a slight brushing between layers was applied.

Microstructural analysis of these samples reveals no significant differences between the two cases, both having a predominant martensitic structure with evidence of chromium carbides, as seen in Fig. 4. Nevertheless, a notorious difference is observed at the macroscopic level, Fig. 5. The grinded deposited wall is considerably more uniform, especially in what concerns to the width regularity, than the wall deposit without grinding. The higher uniformity phenomenon may be due to the grinding of the deposit surface at the cooling stage, which slightly deforms its shape, accommodating the material to the sides, and probably due to a better wetting characteristic. That uniformity can be seen by the correlation between the total wall width (TWW) and effective wall width (EWW). TWW is the largest width that could be achieved in the deposition and EWW is the actual wall width that can be obtained after machining the part. These parameters allow the study of the deposition geometry, its uniformity and permit an estimation of the material wastage after machining. A considerable difference between TWW and EWW implies a lot of machining and a lower buy-to-fly ratio. Buy-to-fly ratio is defined as the ratio of the weight of raw material used to manufacture the part to the weight of the final part. Smoother and regular surfaces are essential to improve buy-to-fly ratios, which can be especially important when machining hard metal, like the one studied. The deposited UTP AF Robotic 600 wire is associated with high hardness values so it can be difficult to machine, as its machinability is grinding only, and for this reason, the samples had to be EDM cut. Therefore, the smoother the surface of the wall, the less machining time it will be needed to achieve the piece's final shape.

Fig. 4 Identical microstructure for both specimens: **a** middle, **b** right bottom. The areas are marked in Fig. 5. Specimen 27 (left) deposited without slag removal. Specimen 29 (right) grinded for slag removal

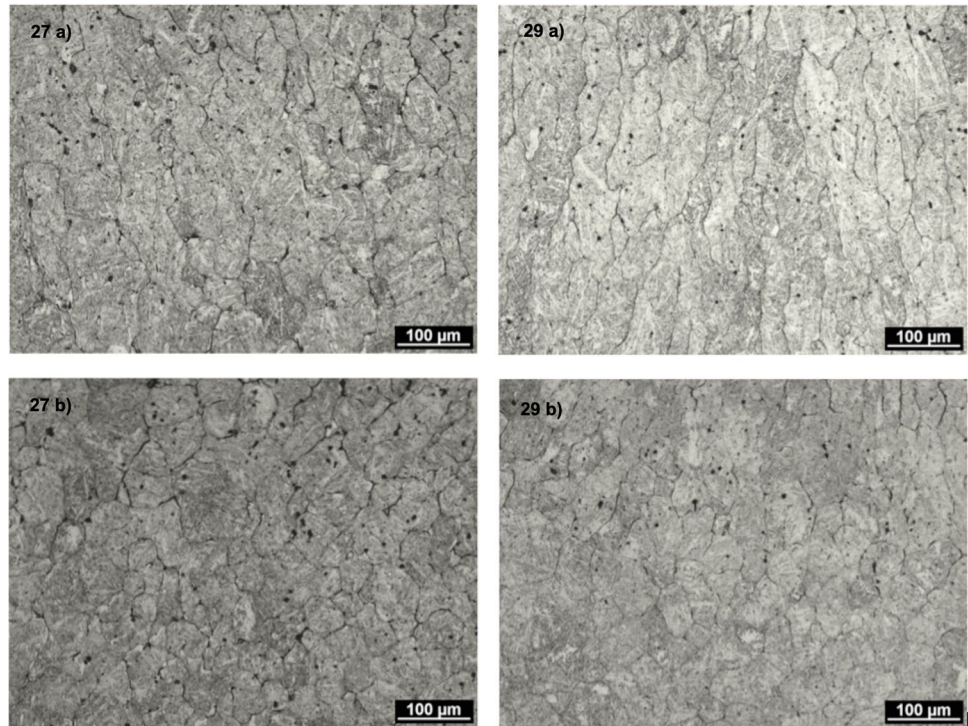
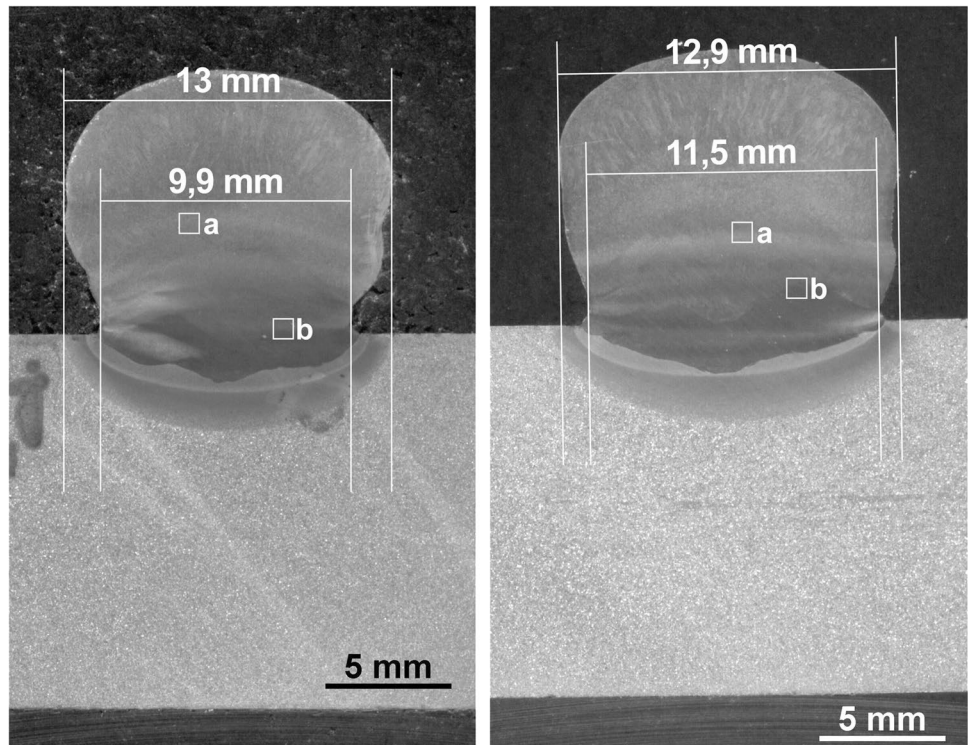


Fig. 5 Left: macro of specimen deposited without slag removal. Right: macro of the grinded specimen, with slag removal



From Fig. 5 it can also be seen that in both samples the first two/three deposited layers have lower width compared to the following ones, result of the higher heat flow through the substrate, meaning that heat extraction is more efficient and the beads shape rapidly. So, for lower side surface wall

variations, different parameters should be used in the first layers.

The hardness measurements made on both walls showed very similar values, being the hardness obtained at the last 6.5 mm of each specimen (corresponding to the 3 last

deposited layers) between 55 and 62 HRC (639 to 803 HV). These values are in accordance with the values given by the manufacturer of the wire for hardfacing applications, for which no more than three layers are usually deposited [14]. Considering the limited number of layers in which this wire is normally applied, and in order to analyze the possibility of producing medium to large parts with this filler, walls with several layers were tested, using the “normal bead” parameters, presented in Table 2.

As result, a 40-layer wall was successfully fabricated, which indicates the possibility of constructing parts entirely from this material. Each layer presents an average height of 3.1 mm and 13 mm of thickness. The analysis performed on this wall indicated that no defects were present in the sample, namely pores, inclusions, or even the evidence of cracks, being the former very common when welding this type of metals.

Microstructural observations and hardness evolution of the 40-wall specimen, similarly to the samples previously presented, show that the surface layer is constituted by martensite with high hardness levels, while the other layers have a tempered martensite microstructure with chromium carbides, due to the subsequent thermal cycles. At the sample's macrography (Fig. 6) it is possible to identify darker lines that appear between layers, corresponding to the interface between two layers. This phenomenon appears due to the Heat Affected Zone (HAZ) of each layer, meaning that when depositing another layer on top of a previous one, a HAZ is formed at each layer, heat-treating the metal due to the heat conduction from the molten pool to the former weld bead. Moreover, for the lighter areas, as for the bottom and top part, the heat dissipation is mainly done by conduction through the substrate for the first deposited layers, whereas at the top part more heat is extracted by convection and radiation. As for the middle of the specimen, heat dissipation becomes less effective and heat accumulates in the building direction, as heat from the previous layers is introduced [18]. These different thermal variations and heat extraction differences lead to inhomogeneous material properties and differences in the local microstructure. These differences are traduced in a wide disparity of hardness values that can be justified by the carbide precipitation, formed due to high carbon content (0.45 wt%) that at high temperatures (above

426 °C) reacts with chromium, forming chromium carbide. This precipitation weakens the metal, thus reducing its hardness [19, 20].

These thermal effects change the hardness due to the increase amount of chromium carbide precipitations in certain regions, as a result of the high heat input associated. Hardness measurements made in this specimen showed great variability with a range obtained from 390 to 806 in a Vickers' hardness scale. Values below 639 HV, the lowest hardness given by the manufacturer, occurred frequently. Figure 5 also overlays the hardness measurements along the centerline of the building direction with the macrography, clearly showing that the darker areas present a minor hardness value, compared with the lighter areas.

The effect of heat accumulation on the microstructure can also be seen on the thinner specimens case, where a higher hardness is obtained because of the less heat input and higher cooling rate. However, these specimens also showed shrinkage cavities where the hardness is higher.

3.2 Block fabrication

In order to understand the influence of the deposition strategy, different blocks were produced to test the appearance of defects and the quality of the weld, both superficial and at a microstructural level. Three deposition strategies were implemented for regular beads: oscillation, parallel, and crossed overlap (left figures in Table 3) and two for weaving beads: oscillation and parallel (right figures in Table 3).

For oscillation and parallel deposition, bidirectional deposition was used (Fig. 7a) and for cross overlap deposition, the path adopts the path represented in Fig. 7b and c.

For block deposition, the traditional flat-top overlapping model (FOM) was used to determine the overlapping ratio of the beads (Fig. 8). This model states that to attain a flat deposition surface, the optimal center distance is $d=0.667w$ [21].

However, for the weaving blocks, an overlap of 67% produced an area of valley too high, as the weaving bead shape is different from the regular bead, resulting in an uneven surface. To overcome this problem, an optimal overlap of 55% was experimentally obtained.

Fig. 6 Overlay of the 40-layer specimen's hardness in its macrography

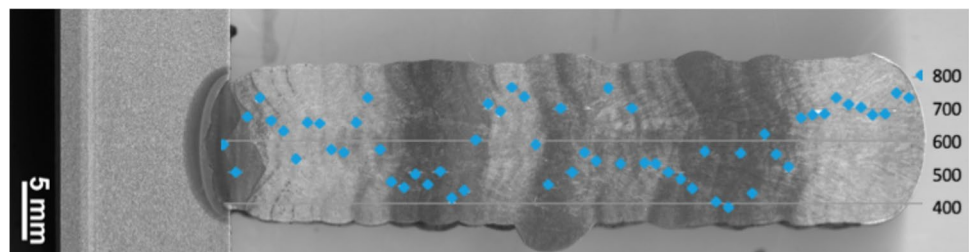
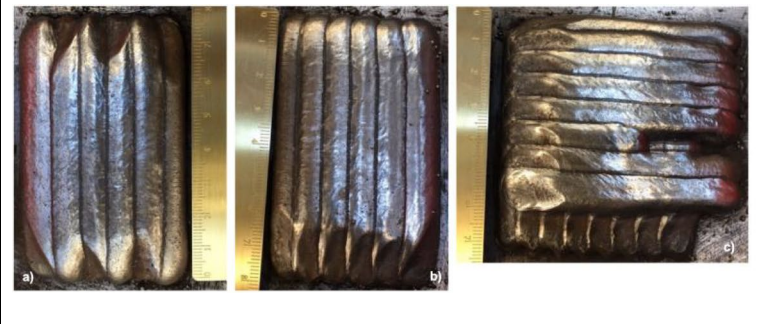
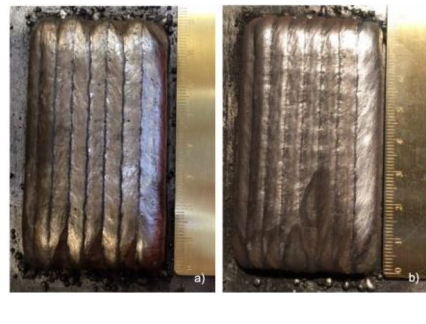


Table 3 Regular bead blocks vs Weaving bead blocks

Regular Beads (a) Oscillated, (b) Parallel, (c) Crossed Overlap	Weaving Beads (a) Oscillated, (b) Parallel
	

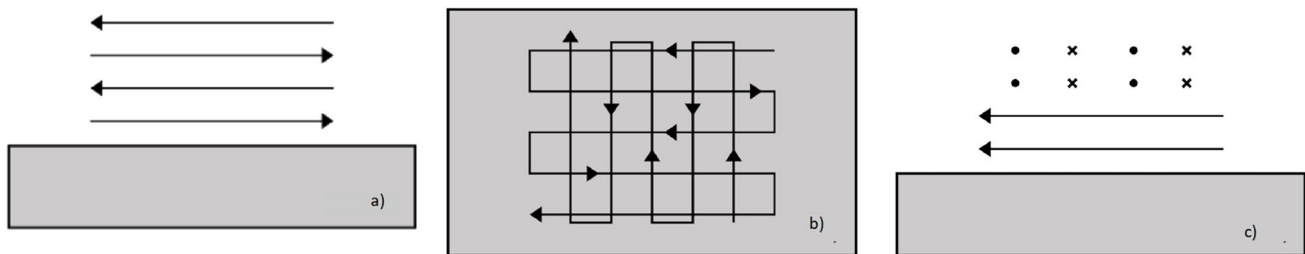


Fig. 7 Bidirectional deposition: **a** Cross overlap deposition: **b** top view, **c** side view

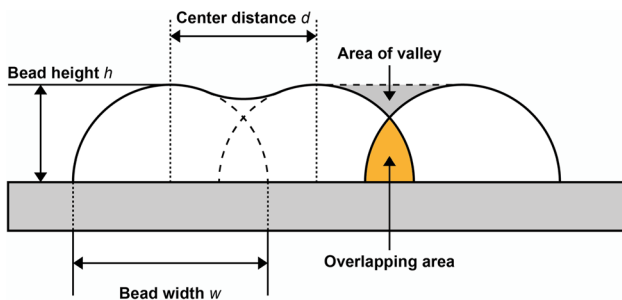


Fig. 8 Overlapping welding beads

During the process deposition, a pre-cleaning step was made between layers to remove the slag, as in block fabrication the slag is expelled to the adjacent area, where the torch will pass to deposit the next bead. So before the succeeding pass, the surface was wire brushed.

Macro and microstructural observations of the blocks produced revealed the presence of cracks and or microcracks [a crack usually only visible under the microscope (50 ×)], and also shrinkage cavities. However, the strategies that gave rise to the lower internal imperfections were the oscillated and parallel regular bead blocks (top figures in Table 4). On the contrary, weaving blocks exhibit severe

cracks (bottom figures in Table 4). Although weaving has proven to produce better results in comparison with regular oscillated and parallel deposition strategies for other wires (for example at [12]), in this case, the flux-cored wire overlays slag to protect the weld bead, so the weaving movement can mix the flux ingredients at the weld pool. In this case, the weaving deposition is not beneficial, only detrimental, facilitating crack formation.

In all the blocks analyzed it was observed, with more or less prominence, that whenever cracks appear, they are located at the transition between beads, at the top and bottom of the sample (top left figure in Table 4). Interdendritic shrinkage cavity is observed at all specimens due to contraction at the deposit superposition, with greater prominence found at the top. Longer cooling time could be used to minimize this effect. If not minimized, shrinkage cavities could expand to what is seen in Fig. 9a), where the former cavity expanded due to the heat received by the following weld bead layer.

The results were compared with the ISO 5817:2014 [22], a standard for fusion-welded joints, which highlighted the severity of the imperfections found. Based on the same standard, the samples produced by oscillated and parallel deposition are considered acceptable for the lowest required quality level in what concerns internal imperfections. Although cracks are not permitted at any quality level, cracks were

Table 4 Macrography of a section from each of the block specimens

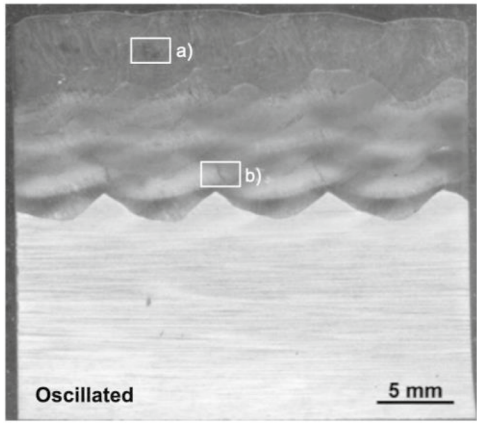
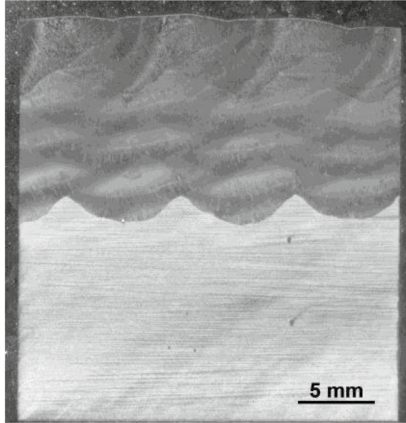
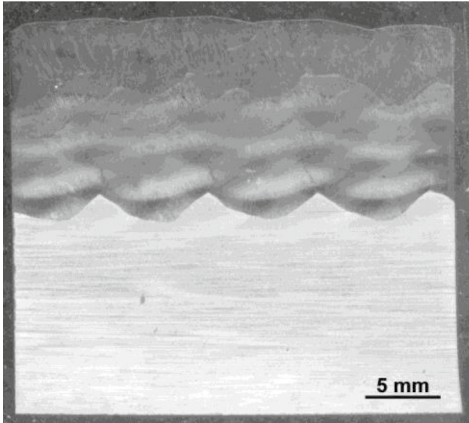
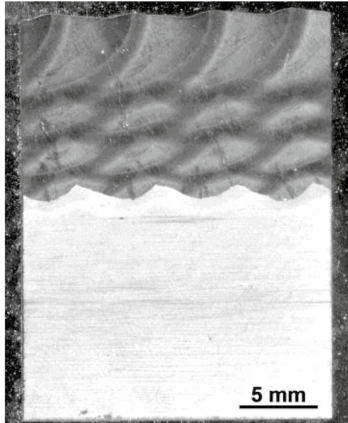
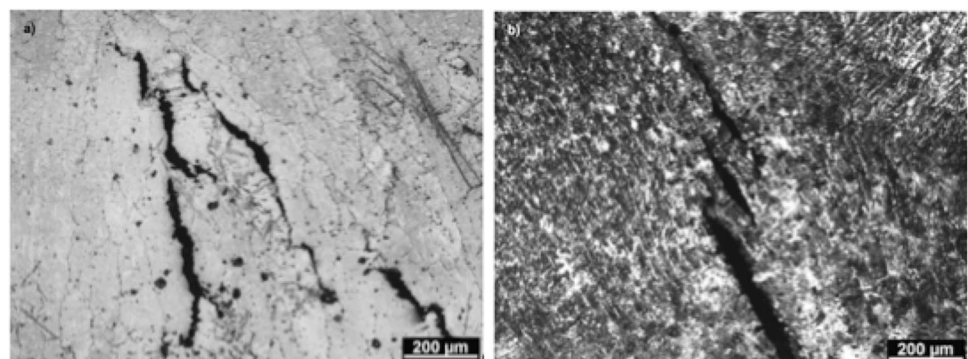
Blocks	Oscillated	Parallel
Regular		
Weaving		

Fig. 9 Micrographic details from the regular oscillated block specimen, from the top left image in Table 4. **a** Shrinkage cavity expanded, **b** crack at the bottom

only found at the bottom (Fig. 9b), arising from the substrate, so this would have to be machined and removed as well as the bottom layers. Regarding the micro-cracks, they are permitted and acceptable at any quality level, depending on the application. Concerning shrinkage cavities, they are only acceptable to the D level, the lowest level, and if it does

not break off the surface; however this issue does not arise. Nonetheless, this standard (ISO 5817:2014) was designed for fusion-welded joints and not for DED applications, but it can point to the severity of the imperfections found.

The microhardness profiles show an overall lower hardness and a more irregular curve, especially for the weaving

blocks that do not even reach 700 HV (see Fig. 10). In multi-layer deposition, the heat transfer not only comes from the top, but also from the deposited sides, creating a more complex cooling cycle, thus having more hardness irregularity.

Nevertheless, no matter the deposition used or even if it is block fabrication or single wall deposition, all of the tested samples presented a higher average hardness than any other part or study samples found in literature, regarding DED-Arc. The highest documented hardness applied to wear applications corresponds to tool steel with an average hardness of 599 HV whereas for oscillated block fabrication the average hardness value is 611 HV [15].

3.3 Two-metal deposition

The possibility of being able to construct a part with more than one metal is desirable because it can allow more design freedom, reduce the costs if a cheaper metal wire is used in locations where high strength is not needed, and coat critical locations with the hardfacing material allowing different properties. It could also be necessary to have a two-metal part by imposition of its requirements or function. Based on this goal, three walls were built, each with eight layers of low carbon steel, on top of which six layers of the hardfacing wire were deposited. To analyze the influence of pre-heating temperature, different pre-heating temperatures (50, 100 and 140 °C) were used before depositing the hardfacing metal, as the first material deposited would cool down to room temperature when changing the wires. Walls were pre-heated with a propane blowtorch and the temperature monitored by a thermocouple, both placed at the middle length of the deposited layers, where the sample would later be cut from. The microstructure and microhardness of the three samples were similar: no differences were observed with the increase of the pre-heating temperature. Furthermore, the interfaces between both metals presented an absence of defects (as seen in Fig. 11), appearing, by visual inspection, a strong and cohesive connection between the two metals, as well as similar hardness along the sample’s height (Fig. 12).

Also, a block was made with oscillation deposition. However, for this case, microanalyses showed cracks with an upper direction arising from the interface between the two different metals likely due to localized uncleaned slag that the melted ER70S-6 wire tends to produce.

Lastly, at the end of the study, a solid part was produced using the two metals. The proposed final part intended to test the conclusions and achievements obtained before. It was built with a stair geometry of the ER70S-6 wire, coated with the hardfacing metal to form a rectangular geometry at the end, as exemplified by Fig. 13. Two layers compose each stair.

For this part, parallel deposition strategy was used, as it was the one that provided the least number of defects in block fabrication, generating a more even and balanced profile. Occasionally, crossed overlap deposition was used. The progression can be seen in Fig. 14. No pre-heating temperature was used between the interface of the two metals.

4 Conclusions

The applicability of a hardfacing flux-cored wire, a wire never before experimented, was tested for arc directed energy deposition. The progressive testes proved, firstly, with the deposition of a 40-layer wall, that this wire can be applied to a greater amount of layers, not only for coating but also for AM purposes; secondly, although some micro-cracks were found in block fabrication, they are acceptable and a solid part can be deposited; thirdly, the deposition of two compatible metals, however more challenging, can be done.

The posterior tests employed to the samples produced, namely the micrography and the microhardness tests, lead to the following conclusions:

- A satisfactory range of bead thickness was obtained, and they were the result of different parameter combinations.
- It was not possible, with the performed parameter optimization, to surpass the higher deposition rate found in the

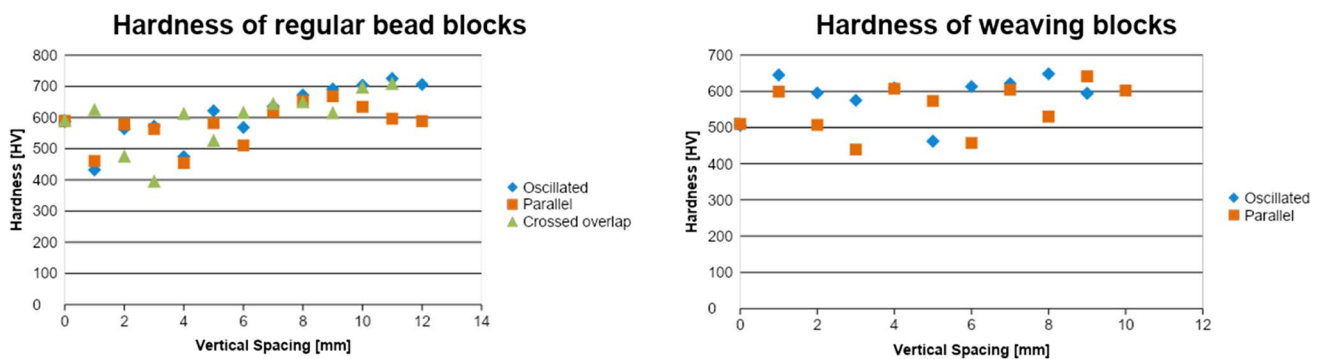
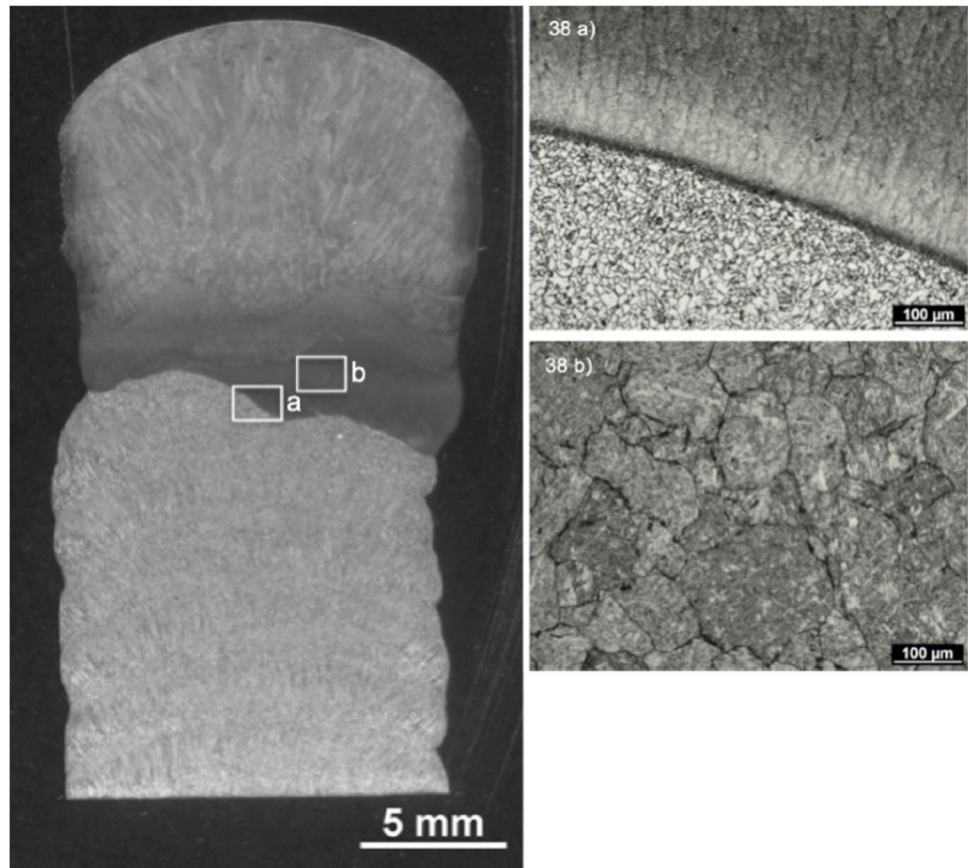


Fig. 10 Hardness comparison between regular and weaving blocks

Fig. 11 Macro (left) and micrographies (right) of a section of a bi-metal deposit, where it can be seen the absence of defects (being the low carbon steel the bottom deposited material, above which the hardfacing metal was deposited)



literature for DED-Arc (5 kg/h for steel) [4]. However, this is a rough comparison as the studied wire presents a different density than the one found in literature, and further experiments with higher WFS could lead to a higher deposition rate.

- For a bigger thermal delivery, more waiting time was needed in order for the slag to come off.
- Slag removal by a grinding machine did not modify the microstructure of the sample, but it changed its geometry, smoothing the side waviness of the wall and reducing the

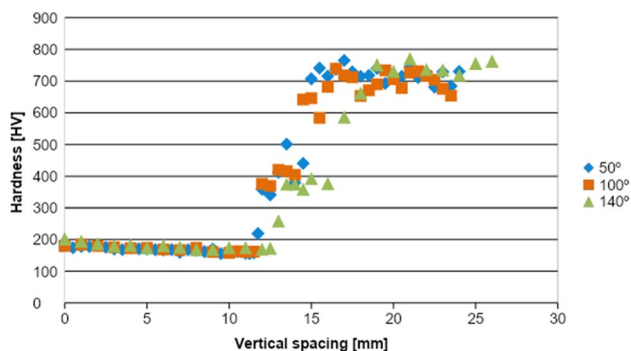


Fig. 12 Hardness of the two-metal deposits with different pre-heating temperatures

side waviness considerably, thus reducing the material waste when machining. This measure proved especially interesting when applied on expensive and hard-to-machine metal wires.

- Higher hardness is observed for areas where the heat dissipation is greater, for instance at the bottom and top of the wall. However, for faster cooling/minor thermal deliveries, cracks are more likely to grow due to interdendritic contractions at the top.
- Weaving deposition strategy is not recommendable for flux-cored wires, as it introduces a variable weld pool, not providing a stable wire flux to the deposit, resulting in severe crack formation. The oscillated and parallel deposition strategies are the best suited for this wire.
- As the cooling profile is more complex at block fabrication, and consequently at the fabrication of a part, the hardness profile is more variable.
- The samples produced in this work presented a higher average hardness (e.g., 611 HV) compared to what was found in literature for both wear applications (599 HV for tool steel discs) and simply documented hardness of tested metals (e.g., 200 HV for stainless steel) [15, 23]. However, work should progress to minimize the hardness variation along the height, bringing the minimum value closest to the maximum.

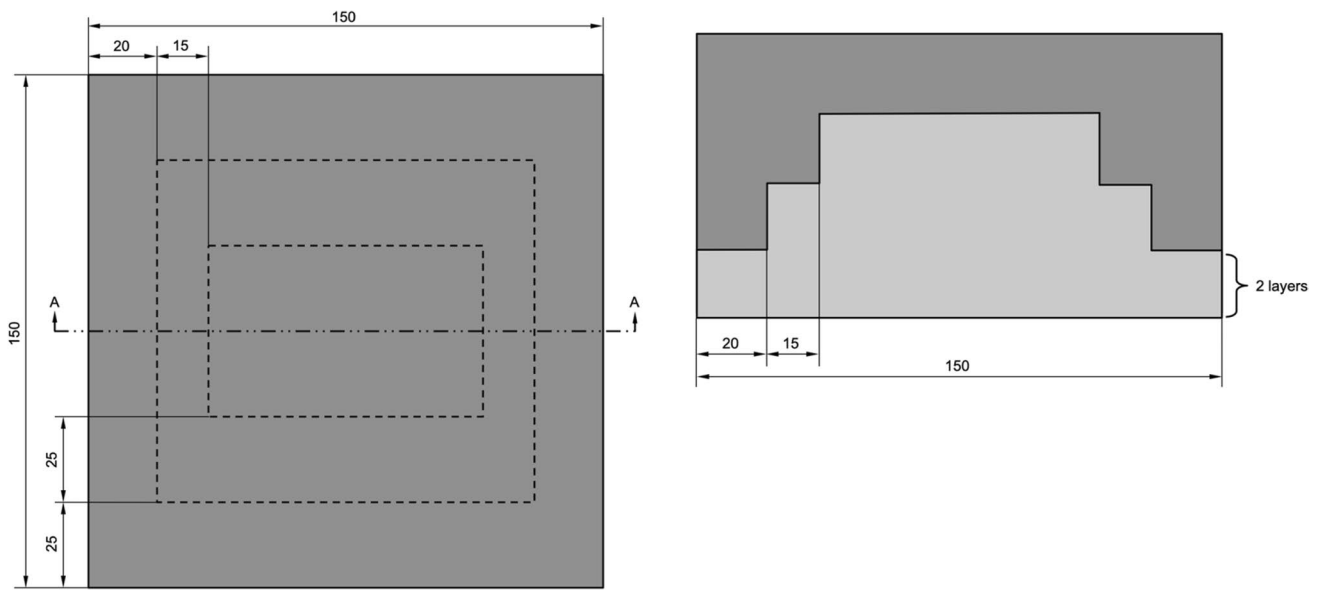
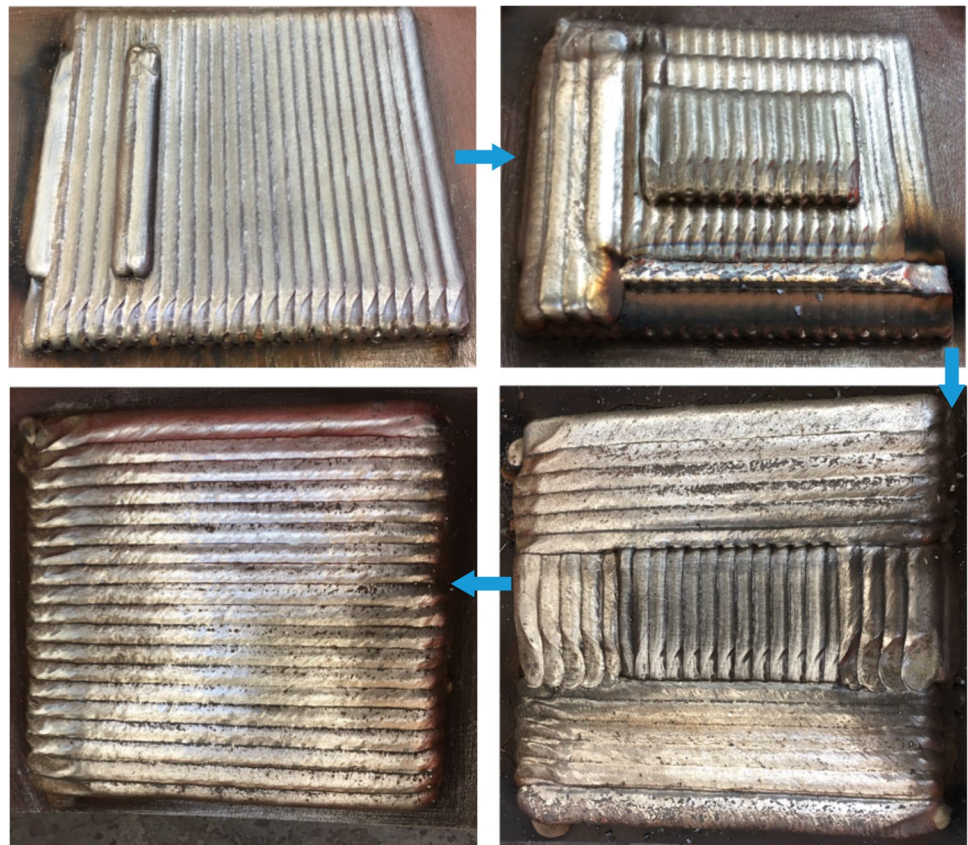


Fig. 13 Left: drawing and measures for the final part. Right: section AA of the final part

Fig. 14 Final part construction



- Regarding the two-metal walls and block deposition, whatever the pre-heating temperature, a strong connection was established between the metals, and it did not affect the microstructure or the hardness of the samples. Crack formation when joining two different

metals can be minimized by a careful pre-cleaning of the surface before applying the following metal and by employing parallel deposition strategy with both wires for an even and balanced distribution of material and residual stresses.

Funding The authors have no relevant financial or non-financial interests to disclose.

Data availability Not applicable.

Code availability Not applicable.

Declarations

Conflict of interest The authors have no conflicts of interest to declare that are relevant to the content of this article.

References

- Williams SW, Martina F, Addison AC, Ding J, Pardal G, Colegrove P (2016) Wire arc additive manufacturing. *Mater Sci Technol* 32(7):641–647
- ISO/ASTM52900-15 (2015) Standard terminology for additive manufacturing—general principles—terminology, ASTM International, West Conshohocken. www.astm.org
- Martina F, Ding J, Williams S, Caballero A, Pardal G, Quintino L (2019) Tandem metal inert gas process for high productivity wire arc additive manufacturing in stainless steel. *Addit Manuf* 25:545–550
- Taberner I, Paskual A, Álvarez P, Suárez A (2018) Study on arc welding processes for high deposition rate additive manufacturing. *Procedia CIRP* 68:358–362
- Colegrove PA, Donoghue J, Martina F, Gu J, Prangnell P, Hönnige J (2017) Application of bulk deformation methods for microstructural and material property improvement and residual stress and distortion control in additively manufactured components. *Scr Mater* 135:111–118
- Silva RJ, Barbosa GF, Carvalho J (2015) Additive manufacturing of metal parts by welding. *IFAC-PapersOnLine* 48:2318–2322
- Geng H, Li J, Xiong J, Lin X, Zhang F (2017) Geometric limitation and tensile properties of wire and arc additive manufacturing 5A06 aluminum alloy parts. *J Mater Eng Perform* 26(2):621–629
- Wang J et al (2018) Characterization of wire arc additively manufactured titanium aluminide functionally graded material: Microstructure, mechanical properties and oxidation behaviour. *Mater Sci Eng A* 734:110–119
- Rodrigues TA, Duarte V, Miranda RM, Santos TG, Oliveira JP (2019) Current status and perspectives on wire and arc additive manufacturing (WAAM). *Materials (Basel)* 12(7):1121
- Wu B et al (2018) A review of the wire arc additive manufacturing of metals: properties, defects and quality improvement. *J Manuf Process* 35:127–159
- Castro e Silva MI (2018) Study of deposition strategies of a wire + arc additive manufactured component. 1–78. <https://www.google.com/url?sa=t&rct=j&q=&esrc=s&source=web&cd=&ved=2ahUKewi73ryEmL3zAhUh4YUKHVPACDcQFnoECAwQAQ&url=https%3A%2F%2Ffenix.tecnico.ulisboa.pt%2FdownloadFile%2F8448200671>
- Xu X, Ding J, Ganguly S, Diao C, Williams S (2018) Preliminary investigation of building strategies of maraging steel bulk material using wire + arc additive manufacture. *J Mater Eng Perform*. <https://doi.org/10.1007/s11665-018-3521-5>
- Guo J, Zhou Y, Liu C, Wu Q, Chen X, Lu J (2016) Wire arc additive manufacturing of AZ31 magnesium alloy: grain refinement by adjusting pulse frequency. *Materials (Basel)* 9(10):823
- Voestalpine Bohler Welding. Utp af robotic 600
- Huttunen-Saarivirta E, Heino V, Vaajoki A, Hakala TJ, Ronkainen H (2019) Wear of additively manufactured tool steel in contact with aluminium alloy. *Wear* 432–433:202934
- Bandyopadhyay A, Heer B (2018) Additive manufacturing of multi-material structures. *Mater Sci Eng R Rep* 129(April):1–16
- Planas I, Santos M (2015) Additive manufacturing of nickel components using CMT process. 90. <https://www.semanticscholar.org/paper/Additive-Manufacturing-of-Nickel-components-using-Pinto/3e55418f1d6c2187df63025e1fa4cf0dfad7bbd#paper-header>
- Cunningham CR, Flynn JM, Shokrani A, Dhokia V, Newman ST (2018) Invited review article: strategies and processes for high quality wire arc additive manufacturing. *Addit Manuf* 22(June):672–686
- ESAB GROUP (2019) Lesson 5—welding filler metals for stainless steels [Online]. Available: https://www.esabna.com/euweb/awtc/lesson5_10.htm (Accessed: 27-Sep-2019)
- Collier J (2019) Carbide precipitation and welding keyway [Online]. Available: <http://www.weldingtipsandtricks.com/carbide-precipitation.html> (Accessed: 27-Sep-2019)
- Ding D, Pan Z, Cuiuri D, Li H (2015) A multi-bead overlapping model for robotic wire and arc additive manufacturing (WAAM). *Robot Comput Integr Manuf* 31:101–110
- CEN (2014) ISO 5817:2014 welding—fusion-welded joints in steel, nickel, titanium and their alloys (beam welding excluded)—quality levels for imperfections
- Haden CV, Zeng G, Carter FM, Ruhl C, Krick BA, Harlow DG (2017) Wire and arc additive manufactured steel: Tensile and wear properties. *Addit Manuf* 16(2010):115–123

Publisher's Note Springer Nature remains neutral with regard to jurisdictional claims in published maps and institutional affiliations.